Effects of As(III) Binding on β-Hairpin Structure

Danny Ramadan, Daniel J. Cline, Shi Bai, Colin Thorpe, and Joel P. Schneider*

Contribution from the Department of Chemistry and Biochemistry, University of Delaware, Newark, Delaware 19716-2522

Received October 2, 2006; E-mail: schneijp@udel.edu

Abstract: While arsenic(III) compounds can exert profound toxicological and pharmacological effects, their modes of action and, in particular, the structural consequences of their binding to cysteinyl side chains in proteins, remain poorly understood. To gain an understanding of how arsenic binding influences β-structure, pairs of cysteines were introduced into a model monomeric β-hairpin to yield a family of peptides such that coordination occurs either across the strands or within the same strand of the β-hairpin. Circular dichroism, NMR, UV−vis spectroscopy, and rapid-reaction studies were used to characterize the binding of monomethylarsonous acid or *p*-succinylamidephenyl arsenoxide (PSAO) to these peptides. Placement of cysteines at non-hydrogen bond (NHB) positions across the β-hairpin, such that they occupy the same face of the sheet, was found to enhance the structure as assessed by CD. Cross-strand cysteine residues that project on opposite faces close to the termini of the hairpin can still bind arsenic tightly and show modestly increased β-sheet content. NMR and modeling studies suggest that arsenic can be accommodated at this locus without disrupting the core interactions stabilizing the turn. However, As(III) binding to nonopposed cysteines, or to cysteines at HB and NHB positions along one strand of the hairpin, caused loss of structure. UV−vis titrations show that all these hairpin peptides bind PSAO stoichiometrically with K_d values from 13 to 106 nM. Further, binding is moderately rapid, with second-order rate constants for association of 10 000−22 000 $M^{-1} s^{-1}$ irrespective of the placement of the cysteines within the hairpin and the consequent extent of structural reorganization required as a result of binding. These studies complement recent work with α-helices and further demonstrate that capture of a pair of thiols by As(III) may result in significant changes in local secondary structure in the protein targets of these potent bioactive agents.

Introduction

Recognized as both a potent toxin[1] and chemotherapeutic,[2] trivalent arsenic can profoundly alter intra- and extracellular processes. The biological effects of As(III) stem, in part, from the avidity of monoalkylated derivatives for closely spaced thiols, e.g.,

$$R-As(OH)_2 + Protein-(SH)_2 \rightarrow$$
$$Protein-(S-)_2As-R + 2 H_2O$$
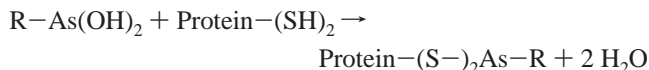
This facile reaction rationalizes the inhibition of a number of key redox enzymes which present a pair of closely spaced thiols to As(III) species. For example, pyruvate dehydrogenase is completely inhibited by monomethylarsonous acid ($CH_3As-(OH)_2$).[3] In addition, glutathione reductase[4] and thioredoxin reductase,[5] enzymes involved in the maintenance of cellular redox poise, are also inhibited by arsenicals.

Although arsenic is normally thought of as a toxin, arsenic trioxide (As_2O_3) is finding use in the treatment of acute promyelocytic leukemia.[2,6−8] Here, arsenic-induced apoptosis may involve both NADPH oxidase inhibition[6] and agonistic effects toward adenine nucleotide translocase.[9] Monoalkylated arsenic(III) species have also been used as fluorescent probes[10] and modulators of angiogenesis.[11]

An important issue concerning the biological effects of arsenic is the extent to which protein conformational changes accompany binding. For example, complexation of As(III) might sequester a pair of catalytically critical cysteine residues with only minimal perturbation of backbone structure. Alternatively, given the large stability constants of alkyldithiol arsenicals,[12]

(1) Hughes, M. F. *Toxicol. Lett.* **2002**, *133* (1), 1−16.
(2) Soignet, S. L.; Maslak, P.; Wang, Z. G.; Jhanwar, S.; Calleja, E.; Dardashti, L. J.; Corso, D.; DeBlasio, A.; Gabrilove, J.; Scheinberg, D. A.; Pandolfi, P. P.; Warrell, R. P. *N. Engl. J. Med.* **1998**, *339* (19), 1341−8.
(3) Petrick, J. S.; Bhumasamudram, J.; Mash, E. A.; Aposhian, H. V. *Chem. Res. Toxicol.* **2001**, *14* (6), 651−656.
(4) Cullen, W. R.; Styblo, M.; Serves, S. V.; Thomas, D. S. *Chem. Res. Toxicol.* **1997**, *10* (1), 27−33.
(5) Lin, S.; Cullen, W. R.; Thomas, D. J. *Chem. Res. Toxicol.* **1999**, *12* (10), 924−930.

(6) Chou, W. C.; Jie, C.; Kenedy, A. A.; Jones, R. J.; Trush, M. A.; Dang, C. V. *Proc. Natl. Acad. Sci. U.S.A.* **2004**, *101* (13), 4578−83.
(7) Miller, W. H., Jr.; Schipper, H. M.; Lee, J. S.; Singer, J.; Waxman, S. *Cancer Res.* **2002**, *62* (14), 3893−903.
(8) Chen, Z.; Shen, Z. X.; Shi, Z. Z.; Fang, J.; Gu, B. W.; Li, J. M.; Zhu, Y. M.; Shi, J. Y.; Zheng, P. Z.; Yan, H.; Liu, Y. F.; Chen, Y.; Shen, Y.; Wu, W.; Tang, W.; Waxman, S.; DeThe, H.; Wang, Z. Y.; Chen, S. J. *Proc. Natl. Acad. Sci. U.S.A.* **2004**, *101* (15), 5328−35.
(9) Belzacq, A. S.; El Hamel, C.; Vieira, H. L. A.; Cohen, I.; Haouzi, D.; Metivier, D.; Marchetti, P.; Brenner, C.; Kroemer, G. *Oncogene* **2001**, *20* (52), 7579−7587.
(10) Griffin, B. A.; Adams, S. R.; Tsien, R. Y. *Science* **1998**, *281*, 269−272.
(11) Don, A. S.; Kisker, O.; Dilda, P.; Donoghue, N.; Zhao, X.; Decollogne, S.; Creighton, B.; Flynn, E.; Folkman, J.; Hogg, P. J. *Cancer Cell* **2003**, *3* (5), 497−509.
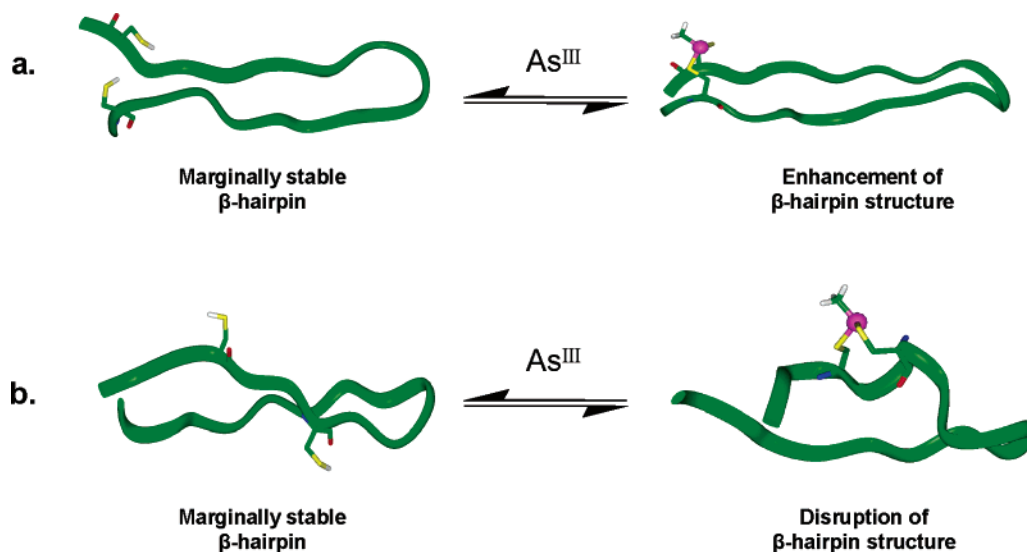(12) Spouches, A. M.; Kruszyna, H. G.; Rich, A. M.; Wilcox, D. E. *Inorg. Chem.* **2005**, *44* (8), 2964−2972.

Figure 1. Schematic representation of As(III) binding to juxtaposed dithiols of model β-hairpins. (a) Enhancement or (b) disruption of the hairpin depends on the sequential arrangement of cysteine residues.

binding of As(III) might induce global changes in protein structure and consequent loss of biological activity.

Hence we seek to understand how arsenic binding influences the conformations of individual secondary structural elements of proteins. We began by studying monomeric α-helices that contain pairs of cysteine residues in varying sequential order and general location within the helix.[13] These helices bind one equivalent of monomethylarsonous acid forming monoalkyl-dithioarsine chelates. Irrespective of their location to one another in sequence space, or their global location with the helix, cysteine side chains bound arsenic relatively quickly[13] affording chelates with low nanomolar dissociation constants. Importantly, binding occurs with concomitant alteration of the helical backbone for nearly all of the cysteine-containing peptides studied. A notable exception to this trend are helices that contain cysteines in i and $i + 4$ sequential positions; here, As(III) binding promotes the fold. In addition, other researchers have documented the ability of As(III) to stabilize three-helix bundles despite a pH favored coiled-coil conformation.[14] These data suggest that arsenic will bind to juxtaposed thiols irrespective of their disposition in the native fold often resulting in perturbations of local backbone structure or even aggregation state.

Encouraged by our results using model α-helices, we now further our evaluation of arsenic binding on another prominent secondary structure motif encountered in proteins, the β-hairpin: two β-strands joined by a short turn region such that the strands are oriented in an antiparallel fashion.[15] Herein, four model hairpins are prepared that incorporate two cysteine residues at different sequential positions. As a result, each peptide displays thiol side chains from the hairpin backbone with a unique spatial presentation. Arsenic binding to each of the peptides should either favor or disfavor the existing secondary structure depending on thiol presentation, Figure 1. These studies provide insight into the structural consequences

of arsenic binding to thiols contained within hairpin structure of native proteins.

In naturally occurring proteins, hairpins contain antiparallel β-strands whose lengths range between 2 and 12 residues.[16,17] The turn geometries observed in β-hairpins are dictated by the dihedral angles (θ, ψ) of the $i + 1$ and $i + 2$ residues of the turn sequence.[18,19] A statistical survey of naturally occurring proteins reveals that certain turns, such as type I and type II, are encountered more frequently in all types of supersecondary structure.[18,20] However, when this survey is limited to β-hairpins in proteins, the mirror image turn types, type I' (83%) and II' (50%), predominate.[20] This turn preference arises from complementarities between turn twist and the natural twist observed in antiparallel β-sheets.[15,18,20] Globally, the β-hairpin is a prominent fold among globular proteins. In an analysis of 50 protein structures (spanning prokaryotes and eukaryotes), Thornton and Sibanda elucidated 255 occurrences of the fold with protein function ranging from protease activity to electron transport.[21]

Ongoing work in the protein design field is helping to establish many of the main determinants that define β-hairpin stability.[17,22–30] Enabling these studies are small model hairpins whose folded structures are robust enough to allow alteration

(13) Cline, D. J.; Thorpe, C.; Schneider, J. P. *J. Am. Chem. Soc.* **2003**, *125* (10), 2923−9.
(14) Farrer, B. T.; McClure, C. P.; Penner-Hahn, J. E.; Pecoraro, V. L. *Inorg. Chem.* **2000**, *39* (24), 5422−3.
(15) Richardson, J. S. *Adv. Protein Chem.* **1981**, *34*, 168−330.
(16) Kabsch, W.; Sander, C. *Biopolymers* **1983**, *22*, 2577−2637.
(17) Gunasekaran, K.; Ramakrishnan, C.; Balaram, P. *Protein Eng.* **1997**, *10* (10), 1131−1141.
(18) Wilmot, C. M.; Thornton, J. M. *J. Mol. Biol.* **1988**, *203*, 221−232.
(19) Hutchinson, E. G.; Thornton, J. M. *Protein Sci.* **1994**, *3* (12), 2207−2216.
(20) Sibanda, B. L.; Thornton, J. M. *Nature* **1985**, *316*, 170−174.
(21) Sibanda, B. L.; Thornton, J. M. *J. Mol. Biol.* **1993**, *229*, 428−447.
(22) Espinosa, J. F.; Munoz, V.; Gellman, S. H. *J. Mol. Biol.* **2001**, *306*, 397−402.
(23) Griffiths-Jones, S. R.; Maynard, A. J.; Searle, M. S. *J. Mol. Biol.* **1999**, *292*, 1051−1069.
(24) Haque, T. S.; Little, J. C.; Gellman, S. H. *J. Am. Chem. Soc.* **1996**, *118*, 6975−6985.
(25) Jourdan, M.; Griffiths-Jones, S. R.; Searle, M. S. *Eur. J. Biochem.* **2000**, *267*, 3539−3548.
(26) Ramirez-Alvarado, M.; Blanco, F. J.; Serrano, L. *Nat. Struct. Biol.* **1996**, *3* (7), 604−612.
(27) Russell, S. J.; Cochran, A. G. *J. Am. Chem. Soc.* **2000**, *122*, 12600−12601.
(28) Maynard, A. J.; Sharman, G. J.; Searle, M. S. *J. Am. Chem. Soc.* **1998**, *120* (9), 1996−2007.
(29) Tatko, C. D.; Waters, M. L. *J. Amer. Chem. Soc.* **2002**, *124* (32), 9372−9373.
(30) Hughes, R. M.; Waters, M. L. *Curr. Opin. Struct. Biol.* **2006**, *16*, 514−524.

Table 1[a]
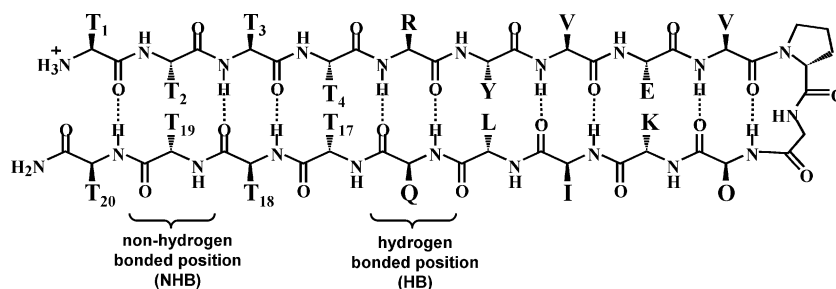
peptide	sequence	Cys positions	K_d (nM)	k_{on} (M^{-1} s^{-1})
1	TCTTRYVEV^{D}PGOKILQTTCT−NH$_2$	NHB/NHB	32 (4)	16 190 (84)
2	TTCTRYVEV^{D}PGOKILQCTTT−NH$_2$	HB/NHB	13 (3)	21 680 (320)
3	TCTTRYVEV^{D}PGOKILCTTTT−NH$_2$	NHB/HB	52 (5)	10 310 (160)
4	TTTCRYCEV^{D}PGOKILQTTTT−NH$_2$	NHB/HB	106 (8)	16 440 (100)
5	TTTTRYVEV^{D}PGOKILQTTTT−NH$_2$			

[a] Standard errors for the dissociation constants (K_d) and the second-order rate constants (k_{on}) for arsenic binding are given in parentheses.

in sequence.[21,22,25,31,32] For example, a 20 residue peptide designed by Gellman et al.[33] adopts a moderately stable (84% folded via δ_{aH} data) monomeric hairpin in aqueous solution; a type II′ central turn composed of ^{D}Pro-Gly connects two strand regions, each of which displays a repeat of four threonine residues at their termini, Table 1 (peptide **5**). Amino acid substitutions made at the threonine-rich regions of this peptide results in measurable changes in hairpin structure.[33,34] Herein, we incorporate two cysteine residues within the strand termini of model hairpin **5** to evaluate the binding affinity, rate, and structural effects of As(III) ligation to cysteine thiols located at different sequential and spatial positions within the hairpin (Table 1).

Peptide **1** incorporates two cysteine residues at positions 2 and 19. Each cysteine residue is contained on a distinct β-strand, directly opposing each other in the folded hairpin. Both residues occupy non-hydrogen bonded positions with the hairpin; amino acids located at non-hydrogen bonded positions do not make intramolecular hydrogen bonds between opposing strands, Table 1. Statistical analysis of proteins that contain disulfide bonds between antiparallel β-strands shows that cysteine residues prefer to occupy non-hydrogen bonded positions on opposing strands, where the cysteine side chains are projected toward the same face of the sheet, adopting χ_1 rotamers conducive to disulfide bond formation.[35,36] We envisioned that As(III) binding to peptide **1** would be a facile event that could result in enhancement of the β-hairpin structure since the ligating thiols are located on the same face of the hairpin in close spatial proximity. Peptides **2** and **3** were designed to establish whether arsenic binding could disrupt the hydrogen bond network of the β-hairpin. Peptide **2** contains an N-terminal cysteine residue at hydrogen bonded position 3 and a C-terminal cysteine at non-hydrogen bonded position 17. In this scenario, the two cysteine side chains are projected on opposite faces of the hairpin. Arsenic(III) binding to peptide **2** would occur across the hairpin

and should result in a complex where the arsenic atom is positioned near the center of the hairpin, disrupting the intramolecular hydrogen bond network. Similarly, peptide **3** also contains cysteine residues whose side chains project toward opposite faces on the hairpin; however, the two residues are spatially located farther apart from each other. In this scenario, As(III) binding, if possible, should lead to gross changes in backbone conformation. Last, peptide **4** contains a Cys-Xaa-Xaa-Cys motif where both cysteine residues reside in a single strand projecting their side chains toward opposite faces of the hairpin. This sequential motif is commonly found in redox active proteins.[37] Although, in this class of proteins, the two cysteines are typically contained within a helix-loop motif, peptide **4** will provide general insight into the propensity this ubiquitous sequential arrangement of cysteines has toward arsenic binding regardless of inherent structure.

Materials and Methods

Trifluoroacetic acid (TFA), 1,3-bis[tris(hydroxymethyl)methylamino]-propane (BTP), ethylenediaminetetraacetic acid (EDTA), piperidine, thioanisole, ethanedithiol, and anisole were purchased from Sigma. Tris-(2-carboxyethyl)phosphine (TCEP-HCl) was purchased from Pierce. Methyldiiodoarsine was prepared as described by Millar et al.,[38] and *p*-aminophenyl arsenoxide (PAO), as described by Stevenson et al.[39] PSAO (*p*-succinylamidephenyl arsenoxide) was prepared as outlined by Cline et al.[13] Fmoc amide resin was purchased from Novabiochem. The appropriate side-chain protected Fmoc amino acids, 2-(1*H*-benzotriazole-1-yl)-1,1,3,3-tetramethyluronium hexafluorophosphate (HBTU), and 1-hydroxybenzotriazole (HOBT) were purchased from Novabiochem. HPLC solvents consisted of solvent A (0.1% TFA in water) and solvent B (90% acetonitrile, 10% water, and 0.1% TFA).

Peptide Synthesis. Peptides **1** through **5** were synthesized on an ABI 433A peptide synthesizer by standard solid-phase peptide synthesis methodology using Fmoc-protected amino acids with appropriate side-chain protecting groups, Rink amide HMBA resin, and HBTU/HOBT activation. Peptides were cleaved with concomitant side chain deprotection using trifluoroacetic acid/thioanisole/triisopropylsilane/ethanedithiol/anisole (88:5:3:2:2). Crude peptides were dissolved to 1 mg/mL in ammonium acetate (0.1 M, pH 7.0) containing 10 equiv of TCEP

(31) Ramirez-Alvarado, M.; Blanco, F. J.; Niemann, H.; Serrano, L. *J. Mol. Biol.* **1997**, *273*, 898−912.
(32) Russell, S. J.; Blandl, T.; Skelton, N. J.; Cochran, A. G. *J. Am. Chem. Soc.* **2002**, *125*, 388−395.
(33) Stanger, H. E.; Syud, F. A.; Espinosa, J. F.; Giriat, I.; Muir, T.; Gellman, S. H. *Proc. Natl. Acad. Sci. U.S.A.* **2001**, *98* (21), 12015−20.
(34) Waters, M. L.; Kiehna, S. E. *Protein Sci.* **2003**, *12*, 2657−2667.
(35) Harrison, P. M.; Sternberg, M. J. E. *J. Mol. Biol.* **1996**, *264*, 603−623.
(36) Srinivasan, N.; Sowdhamini, R.; Ramakrishnan, C.; Balaram, P. *Int. J. Pept. Protein Res.* **1990**, *36*, 147−155.
(37) Fomenko, D. E.; Gladyshev, V. N. *Biochemistry* **2004**, *42* (38), 11214−11225.
(38) Heaney, H.; Heinekey, D. M.; Fernelius, W. C.; Millar, I. T. *Inorg. Synth.* **1960**, *6*, 113−115.
(39) Stevenson, K. J.; Hale, G.; Perham, R. N. *Biochemistry* **1978**, *17* (11), 2189−2192.

and reduced under a nitrogen atmosphere prior to purification. Reduced peptides were purified by RP-HPLC on a Grace-Vydac C-18 peptide/protein preparative column using a linear gradient of 0% to 17% B over 10 min, followed by an additional gradient from 17% to 37% B over 40 min; all peptides eluted around 30 min. MALDI-TOF-MS was used to assess the identity and purity of the β-hairpin peptides using an α-cyano-4-hydroxycinnamic acid (Sigma) matrix: peptides **1**−**2** calculated $(M + H)^+ = 2227.2$, found **1**: 2227.0, **2**: 2227.5; peptide **3** calculated $(M + H)^+ = 2200.1$, found 2199.6; peptide **4** calculated $(M + H)^+ = 2229.1$, found 2229.4; peptide **5** calculated $(M + H)^+ = 2223.2$, found 2223.3.

For comparative studies, peptides **1**−**4** were oxidized according to the method of Cline et al.[40] and purified by HPLC using the same preparative gradient as that for the reduced peptides. Identity and purity of the oxidized peptides were assessed by MALDI-TOF mass spectroscopy: Oxidized peptides **1**−**2** calculated $(M + H)^+ = 2225.1$, found **1**: 2224.8, **2**: 2224.8; oxidized peptide **3** calculated $(M + H)^+ = 2198.1$, found 2197.9; oxidized peptide **4** calculated $(M + H)^+ = 2227.7$, found 2227.1.

Circular Dichroism Studies. CD spectra of oxidized, reduced, As-(III) bound peptides **1**−**4** and the control peptide **5** were collected on a Jasco 810 spectropolarimeter at 4 °C. Wavelength spectra of 100 μM solutions of reduced peptides **1**−**4** and peptide **5** (100 μM in 5 mM KP$_i$, 8 mM KF, pH 6.0) or oxidized peptides **1**−**4** (5 mM KP$_i$, 8 mM KF, pH 6.0) were measured in the absence and presence of 1 and 2 equiv of monomethylarsenous acid (MMA) in a 0.1-cm quartz cell. Titration experiments of reduced peptides **1**−**4** were performed manually in a 0.1-cm quartz cell by successive 1 equiv additions of stock MMA (10 mM in Milli-Q water, adjusted to pH 6.0) to 100 μM solutions of reduced hairpin peptides (5 mM KP$_i$, 8 mM KF, pH 6.0). Peptide samples were prepared from stock solutions in water diluted to concentration with the appropriate buffer. The concentrations of peptide stock solutions were determined by tyrosine absorbance at 276 nm ($\epsilon = 1450$ M^{-1} cm^{-1}). Mean residue ellipticity ($[\theta]$) was calculated using the equation $[\theta] = (\theta_{obsd}/10lc)/r$, where θ_{obsd} is the measured ellipticity in millidegrees, l is the length of the cell (cm), c is the concentration (M), and r is the number of residues.

UV Spectroscopic Studies. Titration experiments for peptide **1**−**4** were performed where 0.25 equiv aliquots of *p*-succinylamidephenyl arsenoxide (aqueous stock) were added to a 100 nM solution of peptide (5 mM sodium acetate, 1 mM KF, 30 μM EDTA, 1 mM TCEP, pH 6.0) contained in a 5-cm path length quartz cell. All solutions were helium sparged directly prior to each experiment. Initial peptide solutions were prepared from an aqueous stock solution whose concentration was determined via Ellman's reagent ($\epsilon_{412} = 14\,150$ M^{-1} cm^{-1} for the corresponding thionitrobenzoate ion).[41]

After each PSAO addition, the solution was equilibrated for 20 min. Plots of absorbance (300 nm) versus concentration of PSAO were fit to eq 1 using Prism GraphPad 3.0, where A = observed absorbance, A_o = absorbance of apo-peptide, A_f = absorbance of peptide/ligand complex, P_t = total peptide concentration, K_d = dissociation constant, and L_t = total ligand concentration.

$$A = A_o + (A_f - A_o)\frac{(Pt + Kd + Lt) - \sqrt{(Pt + Kd + Lt)^2 - 4PtLt}}{2Pt} \tag{1}$$

Stopped-Flow Kinetics. A model SF-61 DX2 stopped-flow spectrometer (Hi-Tech Scientific) equipped with a 75-W Superquiet Xenon lamp was used for rapid mixing kinetics experiments. Stock solutions of peptides **1**−**4** and PSAO (pH 7.0, 50 mM Bis-Tris propane, 150 mM NaCl, 0.3 mM EDTA) were mixed rapidly to give final concentra-

tions of 2.5 μM in peptide and 10, 25, or 50 μM in PSAO. Absorbance changes were monitored at 300 nm, and the data were fit to a single-exponential equation using KinetAsyst 3 software. Three data sets were averaged, and the apparent rate constants were plotted versus PSAO concentration to yield the second-order rate constants.

Analytical Ultracentrifugation. Sedimentation equilibrium experiments were performed at 4 °C using a Beckman Instruments XL-I instrument. All peptide samples were prepared to a final concentration of 170 μM in 10 mM potassium phosphate, pH 6.0. Experiments with reduced peptides were supplemented with 1 mM TCEP, pH 6.0 (Pierce). Each sample was spun at 45 000, 52 000, and 60 000 rpm for 35 h, sufficient time for equilibration. All data were fit (IGOR PRO (Wavemetrics, Lake Oswego, OR)) to a single ideal species model:

$$C_r = C_{r0}\, e\left[\frac{\omega^2}{2RT}M(1 - \bar{v}\rho)(r^2 - r_0^2)\right] \tag{2}$$

where C_r = analyte concentration at the radial position, r; C_{r0} = concentration of monomer at the reference radius; ω = angular velocity; $R = 8.314 \times 10^7$ erg/mol·K; T = temperature (277 K); M = monomer molecular weight; v = partial specific volume of the solute; ρ = solvent density; and r and r_o are the variable and reference radii, respectively.

NMR. NMR experiments were performed using a Bruker (Billerica, MA) AVANCE 600 MHz spectrometer operating with either a CryoProbe (Bruker) or a conventional TXI probe. Data were collected at both 295 and 277 K. Samples of reduced Peptide **1** were prepared to a final concentration of 5 mM in 50 mM potassium phosphate with 1 mM TCEP (9:1 H$_2$0/D$_2$0), pH 6.0. Oxidized peptide **1** was prepared in a similar fashion but without TCEP. Arsenic-bound peptide **1** was prepared to a final concentration of 5 mM in 50 mM potassium phosphate (9:1 H$_2$0/D$_2$0), pH 6.0. Water suppression during all heteronuclear and homonuclear experiments used WATERGATE[42] water suppression. Data were collected with 400 increments along the evolution dimension and 2048 data points along the acquisition dimension. The number of scans per increment was 16 for NOESY experiments, 8 for TOCSY experiments, and 4 for HSQC studies. NOESY experiments were performed over a series of mixing times ranging from 100 to 300 ms. Data from the 300 ms mixing time experiments were used in developing NOE diagrams. The sweep width for all NOESY experiments was 7100 Hz in both the acquisition and evolution dimension. NOEs were qualitatively assigned as strong, medium, weak, or very weak, corresponding to 3, 4, 5, and 6 Å, respectively.[43,44] TOCSY spectra were acquired with 80 ms of spin-lock. The spectral window during all TOCSY experiments was 6000 Hz in both the acquisition and evolution dimensions. Phase-sensitive ^{15}N−^{1}H HSQC spectra were acquired via the standard pulse sequence provided by Bruker. Heteronuclear experiments with arsenic-bound species were conducted with a sweep width of 15 000 Hz on the ^{1}H acquisition dimension and 48 000 Hz along the ^{15}N evolution dimension. Alternatively, the spectral window of apo samples was 6000 Hz along the acquisition dimension and 36 000 Hz along the evolution dimension. Data were processed using XWINNMR (Bruker), and assignments were made with assistance from SPARKY.[45] In all cases, cysteine residues could not be uniquely differentiated.

Results and Discussion

Structural Effects of Arsenic Binding. CD spectroscopy was used to investigate secondary structural changes that occur in reduced peptides **1**−**4** upon the addition of monomethylarsonous acid (CH$_3$As(OH)$_2$). Spectra of the reduced apo peptides are

(40) Cline, D. J.; Thorpe, C.; Schneider, J. P. *Anal. Biochem.* **2004**, *335* (1), 168−170.

(41) Eyer, P.; Worken, F.; Kiderlen, D.; Sinko, G.; Stuglin, A.; Simeon-Rudolf, V.; Reiner, E. *Anal. Biochem.* **2003**, *312* (2), 224−227.
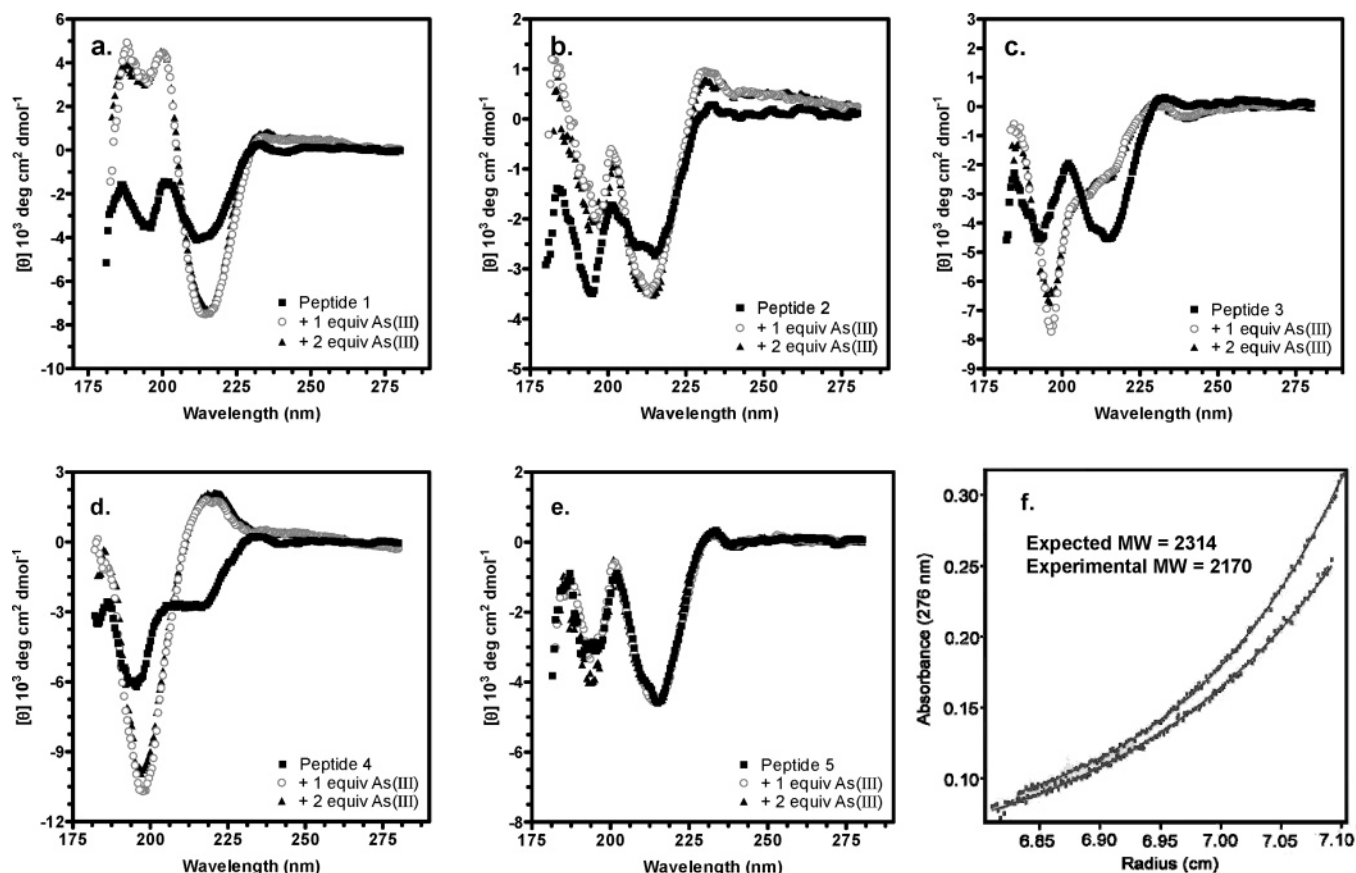
(42) Piotto, M.; Saudek, V.; Sklenar, V. *J. Biomol. NMR* **1992**, *2* (6), 661−5.

(43) Wuthrich, K. *NMR of Proteins and Nucleic Acids*; John Wiley & Sons: New York, 1986.

(44) Evans, J. N. S. *Biomolecular NMR Spectroscopy*; Oxford University Press: Oxford, 1995.

(45) Goddard, T. D.; Kneller, D. G. *SPARKY3*; University of California, San Francisco: 2000.

Figure 2. Far UV−CD of 100 μM solutions of reduced peptides **1**−**5** (a−e, respectively) (pH 6.0, 5 mM potassium phosphate, 8 mM KF) at 4 °C in the absence or presence of monomethylarsonous acid. Sedimentation equilibrium analytical ultracentrifugation of monomethylarsenite bound peptide **1** fit to a single ideal species (52 000 and 60 000 rpm, pH 6.0, 10 mM potassium phosphate, 4 °C).

consistent with the formation of moderately stable β-hairpins, exhibiting mean residue ellipticity minima at 195 and 215 nm ($[\theta]_{195}$ and $[\theta]_{215}$) due to both random coil and β-sheet contributions, respectively. The spectra of apo reduced peptides **1**−**3** closely resemble those of control peptide **5** (Figure 2a−c, e), in good agreement with Gellman's earlier structural assessment of this sequence. Apo-peptide **4** exhibits a spectrum having a greater negative contribution at 195 nm relative to 215 nm, indicative of a slightly less ordered hairpin; this is most likely due to replacing the high β-sheet propensity valine residue at position 7, a position proximal to the turn region of the hairpin, with cysteine, Figure 2d. Addition of 1 equiv of monomethylarsonous acid to peptide **1** resulted in a substantial increase in β-sheet structure as evidenced by the nearly 2-fold increase in negative ellipticity at $[\theta]_{215}$ and concomitant decrease in negative ellipticity at $[\theta]_{195}$.

Further addition of arsenic (2 equiv) resulted in very little change to the CD spectrum, Figure 2a. RP-HPLC analysis of this solution showed the existence of only one species whose molecular weight (MALDI-TOF MS) was consistent with the formation of the anticipated methylarsenite−peptide adduct (e.g., peptide−As−CH₃) (see Supporting Information, S2). Further, the CD spectrum of control peptide **5** under identical solution conditions showed no change upon the addition of As(III), strongly implicating the cysteine residues of peptide **1** in arsenic binding, Figure 2e. Since small hairpins have a propensity to self-assemble, and this event could lead to an apparent increase in β-sheet content as measured by CD,[46] we assessed the

aggregation state of this peptide. The sedimentation equilibrium analytical ultracentrifugation data shown in Figure 2f indicate that the peptide **1**−arsenic complex is monomeric in solution, implying that the metal binding event does not promote self-assembly and that the enhanced β-sheet structure observed by CD resulted from an intramolecular binding event that limits strand end-fraying. NMR spectroscopy was then used to study structural changes resulting from As(III) binding, Figure 3. NOE spectroscopy indicated that apo peptide **1** adopts a β-hairpin conformation as evidenced by strong NOEs among turn-forming residues (i.e., Val9 Hγ−Pro10 Hδ, Pro10 Hα−Gly11 NH, Gly11 NH−Orn12 NH) and cross-strand NOEs defining the antiparallel strand alignment (Thr4 Hβ−Leu15 Hα, Arg5 NH−Gln16 NH, Tyr6 H₂,₆−Ile14 Hβ) with fewer NOES observed at the N- and C-termini, Figure 3a (see Supporting Information, S17). The lack of cross-strand NOEs at the termini of apo-peptide **1** is commensurate with fraying seen at the strand ends of β-hairpins.[33] Surprisingly, when peptide **1** binds As(III), fewer cross-strand NOEs are observed, an apparent contradiction to the aforementioned CD data, Figure 3b. ¹⁵N−¹H HSQC spectra provided insight into this phenomenon. Figure 4a−c show ¹⁵N−¹H HSQC spectra for apo-peptide **1**, methylarsenite-bound peptide **1**, and intramolecularly disulfide bonded peptide **1**, respectively. While the CD spectra of oxidized peptide **1** and methylarsenite peptide **1** appear similar, NMR reveals that the presence of arsenic profoundly alters the chemical environment

(46) Schneider, J. P.; Pochan, D. J.; Ozbas, B.; Rajagopal, K.; Pakstis, L.; Kretsinger, J. *J. Am. Chem. Soc.* **2002**, *124*, 15030−15037.
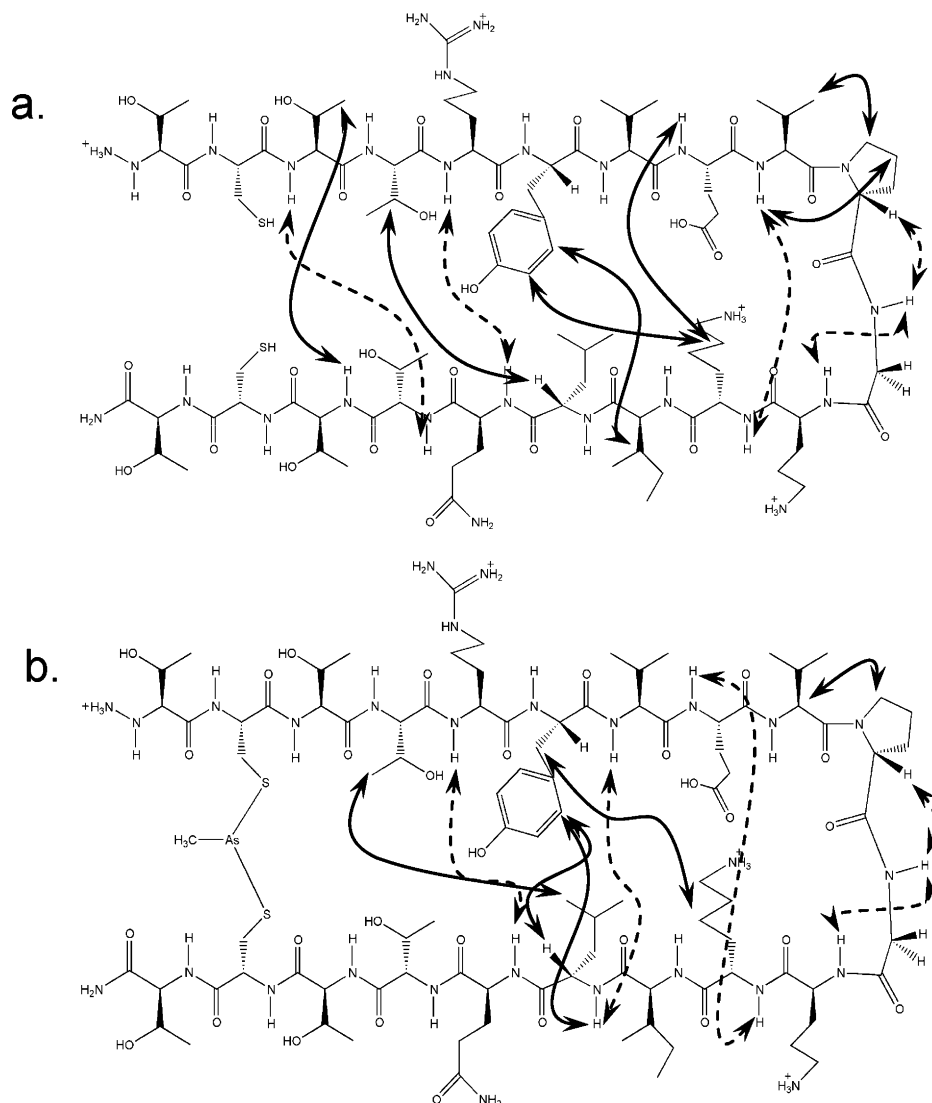
Figure 3. NOEs between cross-strand and turn-forming residues in apo (a) and methylarsenite-bound (b) peptide **1**. NOESY experiments were conducted with 5 mM peptide in 50 mM potassium phosphate, pH 6.0 (9:1 H_2O/D_2O) at 4 °C with 300 ms mixing time. Solid arrows illustrate NOEs involving side chains, and dashed arrows indicate backbone−backbone NOEs.

of the β-hairpin (see Supporting Information for CD of oxidized peptide **1**). Both the apo-reduced and oxidized form of peptide **1** exhibited the expected number of amide resonances while the methylarsenite bound form displays more amide resonances than expected for a 20 amino acid peptide. In our hands, it was impossible to make accurate assignments in the region proximal to the arsenic center in the bound form of peptide **1**. Despite this obstacle, both cross strand NOEs (i.e., Arg5 NH−Gln16 NH, Tyr6 $H_{2,6}$−Leu15 Hα, Val7 NH−Leu15 NH) and NOEs between turn-forming residues (i.e Val9 Hγ−Pro10 Hα, Pro10 Hα−-Gly11 NH, Gly11 NH−Orn12 NH) (Figure 3b and Supporting Information) were readily observable distal to the arsenic atom suggesting that while the peptide retains a β-hairpin conformation, there is a great deal of disorder at both the N- and C-termini leading to multiple conformations. This disorder is most likely due to inversion about the arsenic center[47] resulting in the presence of multiple conformations on the NMR time scale at both 277 and 298 K (data not shown).

(47) Andose, J. D.; Rauk, A.; Mislow, K. *J. Am. Chem. Soc.* **1974**, *96* (22), 6904−6907.

Peptide **2**, which displays its thiol side chains on opposite faces of the folded hairpin, also binds monomethylarsonous acid with 1:1 stoichiometry as evidenced by RP-HPLC and MALDI-TOF MS. Surprisingly, when peptide **2** binds As(III), CD spectroscopy indicates a slight enhancement of the β-sheet structure, Figure 2b. Here, metal binding must occur across the hairpin disrupting the local H-bonding network near the termini. Modeling suggests that arsenic can bind at this locus without perturbation of the overall backbone structure. Importantly, NOEs involving amino acids 9−12 in peptide **2** confirm that the strand registry remains unchanged upon arsenic binding suggesting that the arsenic facilitates binding across the face of the hairpin (see Supporting Information).

CD spectroscopy of reduced peptide **3** reveals that incorporation of two cysteine residues at the expense of Thr2 and Gln16 does not alter the secondary structure with reference to control peptide **5**, Figure 2c and e. Addition of MMA to peptide **3** resulted in a 2-fold loss in mean residue ellipticity at 215 nm as the random coil state is populated at the expense of the β-sheet. Therefore, when cross strand cysteine residues are
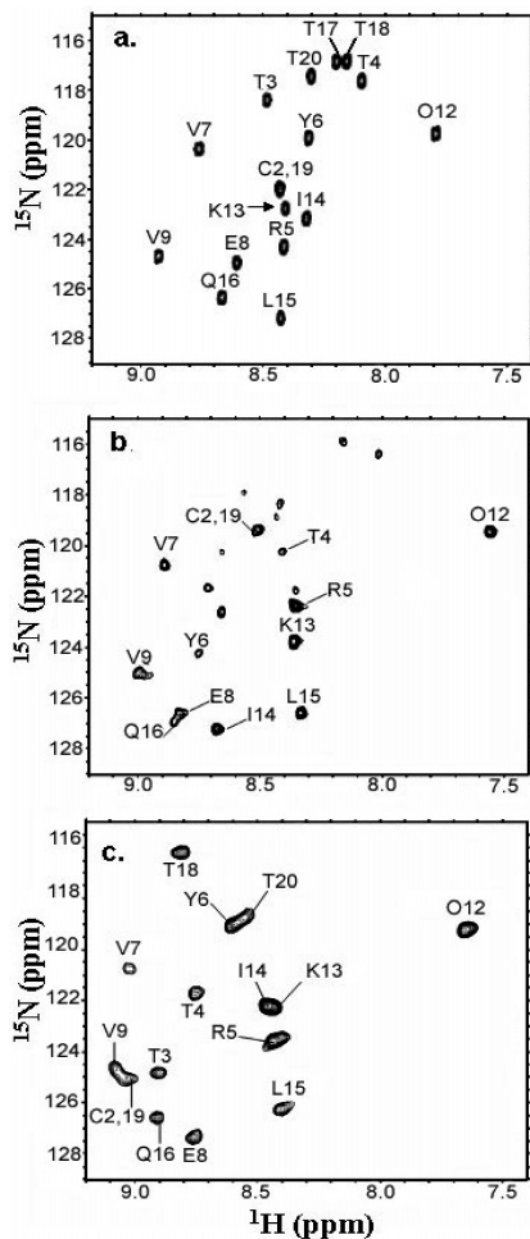
Figure 4. Comparative $^{15}N-^1H$ HSQC spectra of reduced peptide **1** (a), methylarsenite-bound peptide **1** (b), and intramolecularly oxidized peptide **1** (c). Note: In all cases, Gly11 amides resonated outside the plotted region. Samples were prepared in 50 mM potassium phosphate, pH 6.0, 9:1 H$_2$O/D$_2$O with reduced samples supplemented with 1 mM TCEP.

located spatially distal to one another on opposite faces of a β-hairpin, As(III) binding disrupts the secondary structure.

Figure 2d shows that the reduced form of peptide **4** contains less structure compared to control peptide **5**, most likely due to the replacement of a high β-sheet-propensity valine residue with a cysteine at position 7. Consequently, peptide **4** exhibited a dramatic response to the addition of arsenic adopting an alternate conformation inconsistent with either the β-sheet or random coil. The CD spectrum is reminiscent of a reverse turn[48] with an identical spectrum being previously observed by this lab when model α-helices containing cysteines in the i and $i + 3$ positions bind As(III) stoichiometrically.[13] Taken together, this data lend credence to molecular modeling showing (see Supporting

(48) Smith, J. A.; Pease, L. G. *CRC Crit. Rev. Biochem.* **1980**, *8*, 315–399.

Information; S11) that arsenic binds these same-strand cysteines with a total disruption of the hydrogen bond network of the β-hairpin.

Directly following the CD titration, peptide solutions of **1**−**4** were individually injected on an RP-HPLC instrument. Peptide **3** eluted as two components by RP-HPLC, each having identical molecular weights. The same behavior was observed for peptide **4**, while peptides **1**, **2**, and **5** eluted as single components. This data suggest that arsenic-bound **3** and **4** exist as an equilibrium mixture of structural isomers. Reinjection of each isolated peak onto the HPLC results in the reappearance of two peaks with the same relative ratios. The behavior of arsenic-bearing peptides **3** and **4** is most likely due to a slow interconversion of isomers resulting from the known inversion of As(III) compounds at the metal center.[47] Thus, individual CD spectra for the arsenic-bound state of these two peptides represent the contributions from both conformers.

Chelate Stability and Kinetics. Figure 5a shows a representative UV-based titration experiment, where 0.1 μM of reduced peptide was titrated with spectroscopically active *p*-succinylamidephenyl arsenoxide (PSAO). Bound PSAO has an absorption spectrum red-shifted relative to unbound PSAO, and binding can be followed easily at 300 nm.[13] The binding of PSAO to peptides **1**−**4** was tight with K_d values from 13 to 110 nM (Table 1). In our previous work binding arsenic to pairs of cysteine residues in an α-helical context,[13] we obtained comparable dissociation constants (from 20 to 200 nM). For context, Wilcox et al. recently reported dissociation constants for MMA to a variety of small dithiol ligands (such as dithiothreitol and dihydrolipoic acid) between 90 and 1200 nM.[12] Our experiments were performed in the absence of competing monothiols such as glutathione that would be present under physiological conditions. Under these conditions, monothiols may slightly decrease the apparent binding constant of arsenic to dithiol motifs but should not affect the specificity of the binding event.

In order to study the kinetics of arsenic binding we conducted stopped-flow spectroscopic measurements on reduced peptides **1**−**4** under pseudo-first-order conditions (see Figure 5b for representative data). The increase in absorbance at 300 nm is fit to a single exponential, and the resulting apparent first-order rate constants are plotted as a function of PSAO concentration in Figure 5c. Second-order rate constants are presented in Table 1 (see also Supporting Information). In all cases binding is relatively rapid with rate constants from 10 000 to 22 000 M^{-1} s^{-1}. These values are again comparable to our previous results with helices (k_{on} = 11 000−28 000 M^{-1} s^{-1}).[13]

Conclusions

These data complement our previous studies on the binding As(III) species to dicysteine motifs within α-helices. We now conclude that arsenic binding can both favor and disfavor helical and β-hairpin structures depending on the placement of cysteine residues and the plasticity of the secondary structural elements to insertion of a monoalkylated As(III) derivative. However, there is little impact on the dissociation constants for these arsenic(III) chelates even when the cysteines are placed in positions that appear, a priori, unfavorable for binding: e.g., when projecting toward opposite faces of the hairpin, or at i and $i + 1$, $i + 2$, or $i + 3$ positions in an α-helix. Further, the
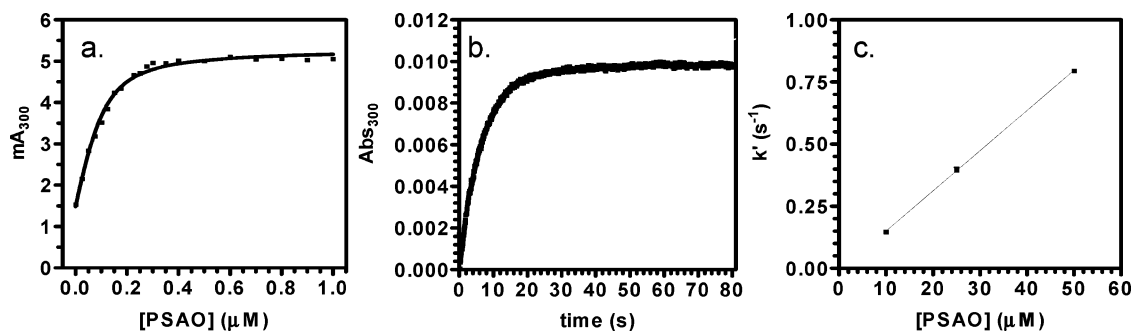
Figure 5. (a) mA_{300} as a function of PSAO concentration for a 0.1 μM solution of peptide **1** (5 mM sodium acetate, 1 mM KF, 30 μM EDTA, 1 mM TCEP); the data are fit to a 1:1 binding stoichiometry affording a K_d of 32 nM. (b) Stopped-flow absorbance measurements mixing 10 μM PSAO with 2.5 μM peptide **1** (final concentration) in 50 mM BTP, 150 mM NaCl, 0.1 mM EDTA, pH 7.0. (c) A second-order rate constant of 16 190 M^{-1} s^{-1} was obtained from a linear fit of apparent rate constants as a function of PSAO concentration (standard errors are listed in Table 1).

rates of association of As(III) to dithiol motifs in environments that would readily accommodate the pyramidal coordination of As(III) with minimal structural reorganization are not significantly different from those instances where binding would promote major disruptions in structure. It appears that the free energy realized from the acquisition of two new As−S bonds overwhelms the structural biases of those dithiol peptides that present initially unfavorable geometries for arsenic binding. As a minimum, we would expect that As(III) binding to dicysteine motifs in proteins will induce local changes in secondary structure without global rearrangement of the protein fold. At the other extreme, folded proteins of marginal stability may suffer major changes in tertiary structure and activity even when the cysteine residues are not directly involved in catalysis. Although the effects of As(III) species are usually interpreted in terms of binding to mature, folded proteins, the insights developed herein may also apply to proteins undergoing folding in the cell. Here, the intermediates along the folding pathway may allow transiently juxtaposed cysteine side chains to be

captured by As(III) species with consequent interference in the acquisition of the native protein fold.

Supporting Information Available: Circular dichroism control titrations of oxidized peptides with respective MALDI-TOF MS and RP-HPLCs, energy minimized structures of reduced and arsenic-bound peptides, dissociation constant determinations, associative rate constant determinations, analytical ultracentrifugation of reduced peptide **1**, tables of NOE intensities observed in apo-reduced, intramolecularly oxidized, and arsenic-bound states of peptide **1**, and NOE intensities observed in the turn region of arsenic-bound peptide **2**. This material is available free of charge via the Internet at http://pubs/acs/org.

JA067068K